On the Use of Thermal Conductive Focusing for Solar Concentration Enhancement

Francisco J. Arias[a,b*]
[b] *Department of Fluid Mechanics, Universitat Politècnica de Catalunya (UPC), Spain. ESEIAAT C/ Colom 11, 08222 Barcelona, Spain and*
[b] *Department of Engineering, University of Cambridge Trumpington Street, Cambridge, CB2 1PZ, United Kingdom*
(Dated: April 22, 2016)

We discuss the possibility for solar concentration enhancement via conductive heat transport. Here, we are concerned, as in orthodox approaches, about maximizing the solar concentration to obtain the highest receiver temperature possible, but with one important difference: In the proposed approach, the solar concentration enhancement is attained not by the use of lenses, mirrors, or funnels (i.e., by optical concentration based on radiative transport), but via thermal conduction, what we call thermal conductive focusing. Among the additional advantages of thermal conductive focusing is the capability to concentrate indistinct direct incidence as well as diffusive radiation. Thus, the concept is especially insensitive to cloudy days and particularly attractive in application to environments with important diffusive components of light. Utilizing a simplified geometrical model, an analytical expression for the temperature and concentration gain at the receiver was derived. The particular application for a parabolic solar trough was analysed. Additional research and development is required to explore the possibilities of solar flux enhancement by thermal conductive focusing as well as the optimization of several variables.

Keywords. *Thermal Concentration, Conductive Heat transfer, Radiative heat transfer, Solar energy*

I. INTRODUCTION

The object of this work is to analyse an approach for solar concentration enhancement to maximise the temperature at the receivers in concentrating solar power systems. Here, contrary to the current approaches based on optical concentration, i.e., based on the use of mirrors, lenses, or funnels, we are interested in attaining a solar concentration enhancement via thermal conductive heat transport, what we call *conductive focusing*.

A. State-of–the-art solar concentration systems

Today, systems for concentration of solar radiation become necessary when high temperatures are desired at the receiver. Such systems, known as concentrating solar power systems, encompass a broad spectrum of familiar technologies such as parabolic troughs, parabolic dishes, power towers, and compound parabolic concentrators. For more thorough discussions of the concentration solar technologies, the reader is referred to the classical books by Lovegrove [1], Francis [2], and Garg & Prakash [3]. Nevertheless, despite the aforementioned myriad of solar concentrator technologies, all of them, in one way or another, are based on the use of lenses, mirrors, or funnels, where the solar concentration is attained by radiative transfer, i.e., by focusing the direct incidence of sunlight beams by reflection and/or refraction of the light.

In this manuscript, we will assess the possibility to boost solar concentration by thermal conduction. As far as the author knows, this idea has not been contemplated before.

II. THERMAL CONDUCTIVE FOCUSING CONCEPT

A. Statement of concept

Thermal conductive focusing may be implemented in solar concentration technology in several ways and many different geometries to do so may be envisaged. However, as a first approximation, and to generalise the theoretical treatment of the concept, the simplest geometry is a slab, which will allow us to identify the variables involved in the performance of thermal conductive focusing as well as the maximum ideal, theoretical values attained.

Because such a slab will act between classical solar collectors and receivers, hereafter, we will refer to this slab as a *transceiver*.

The essentials of a transceiver are depicted in Fig.

*Corresponding author: Tel.: +93 73 98 666; Electronic address: fja30@cam.ac.uk

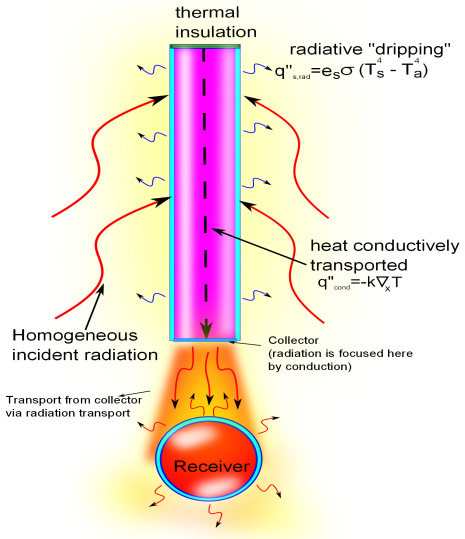

FIG. 1: The thermal transceiver concept

1. The performance of a transceiver is a compromise between the radiative and convective losses being re-emitted into the environment and the effective conductive heat flow being transported to the collector. Both of these factors, thermal leakage, and thermal conduction are determined by the temperature of the transceiver. It might be thought, at first sight, that increasing the transceiver length indefinitely would cause the heat flux at the collector to be increased indefinitely. However, after some careful thought, it is easy to see that increasing the length of the transceiver will result in an increase of its internal temperature and of its thermal losses. It would soon reach a point where it would no longer produce useful heat flux at the collector, i.e., the radiative heat losses at the wall will be larger than the internal conduction heat flow toward the collector.

In addition, the reader should keep in mind that according to the second law of thermodynamics, the source of energy for the transceiver, i.e., the sun, must always be at a higher temperature than the receiver (the whole system). However, there is nothing preventing, at least not from the second law, a collector with a lower temperature than the receiver and yet having heat flow in the direction collector $\longrightarrow$ receiver. Entropy is an extensive magnitude and must be calculated considering the entire system. As Max Planck pointed out early on: *'carefully we must proceed when estimating the entropy of any system from the entropies of its constituents. It is strictly necessary, when dealing with any part of the system, first to ask whether it is possible that any other place in the system there is a coherent part of the system. Otherwise phenomena apparently contradicting the entropy principle might occur in the case of the unexpected mutual action of two sub-systems.'*, [4].

Before developing the theoretical treatment of a transceiver, the reader may perhaps gain some good insights by considering the following analogy. The transceiver could be viewed as the thermal equivalent of a classical hosepipe, where the temperature and heat flux are the equivalents of the pressure and the fluid flow in the hosepipe, respectively. Thus, for a hosepipe, if the pressure (the temperature in the transceiver) increases then the fluid flow at the hosepipe-nozzle (the heat flux at the collector in the transceiver) increases. However, if the pressure in the hosepipe (the temperature in the transceiver) increases beyond a certain threshold, then leakage will appear (radiative losses plus convective losses in the transceiver) and the fluid flow at the hosepipe-nozzle (the heat flux at the collector) attains a maximum value.

Let us consider, for the sake of illustration, the simple transceiver depicted in Fig. 1, but now including its dimensions and several parameters necessary for the theoretical treatment in Fig. 2. Consider a transceiver with a length **x=b**, width **y=l**, and thickness **z=t**. The incident radiative heat, $\mathbf{q}''$ (e.g., the solar irradiation) is being collected in the surface $P \cdot b$ where P is the perimeter of the slab, (in this case, $P = 2l + 2t \approx 2l$). In addition, the top wall boundary of the slab located at **x=0** is thermally isolated and can be considered adiabatic with temperature T_o. On the other hand, the opposite wall, located at **x=b**, is called the 'collector' and has surface $\mathbf{A}_c$ and temperature T_c. The receiver that is facing the collector has a radius **a**, a surface $\mathbf{A}_r$, and is a distance r from the collector wall. Inside, the slab is composed of a material with high thermal conductivity κ and with a surface area $P{\cdot}b$ covered with a selective coating featuring a low emissivity and high absorption, $\bar{\epsilon}_s$. In contrast, the collector features high emissivity, $\bar{\epsilon}_c$. Finally, the receiver is covered with a very low emissivity and high absorption layer, $\bar{\epsilon}_r$.

First, consider a rough calculation of the typical expected Biot number for a transceiver as a preliminary step, before starting our theoretical treatment. This calculation will allow us to apply some simplifying assumptions that will eventually enable us to derive an analytical expression for a coupled radiative-conductive system.

First, we need to identify the thermal losses in the transceiver, which can be radiative (radiative dripping) and/or convective. The radiative dripping at the surface $P \cdot b$ is the heat that is re-emitted radiatively by the surface, and is given by

$$q''_{s,rad} = \bar{\epsilon}_s \sigma (T_s^4 - T_a^4) \quad radiative \quad losses \qquad (1)$$

where σ is the Stefan-Boltzmann constant, T_s the temperature at the surface **s**, T_a the room temperature, and $\bar{\epsilon}_s$ the average emissivity (averaged over temperature and frequencies). Hereafter emissivities are considered to be

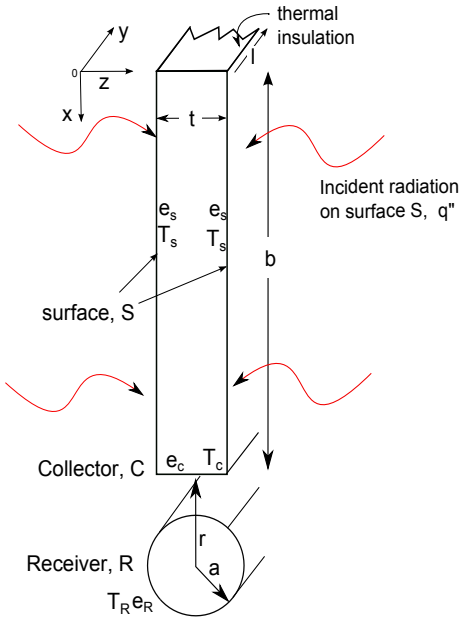

FIG. 2: Physical model for the calculation of heat transmission in the slab

averaged values. On the other hand, the convective losses are calculated as

$$q''_{s,conv} = h_s(T_s - T_a) \quad convective \quad losses \tag{2}$$

where h_s is the convective heat transfer coefficient at the surface s, i.e., surface $P \cdot b$. In the same way, the heat transfer by conduction along the x-axis, (see Fig. 2) is given by

$$q''_{cond,x} = -\kappa \frac{dT}{dx} \tag{3}$$

Now, assuming a room temperature T_a, and a temperature at the surface s T_s, then,

$$q''_{cond,x} \approx -\kappa \frac{T_a - T_s}{b} \tag{4}$$

and thus, the ratio between the thermal losses (both radiative and convective) and the thermal conduction inside the slab can be expressed as

$$\mathbf{Bi} = \frac{\bar{\epsilon}_s \sigma T_s^3}{\frac{\kappa}{b}} \cdot \frac{\left[1 - \Phi^4\right]}{\left[1 - \Phi\right]} + \frac{h_s}{\frac{\kappa}{b}} \tag{5}$$

where

$$\Phi = \frac{T_a}{T_s} \tag{6}$$

Equation (5) can be rewritten in a more compact way as function of the Biot numbers:

$$\mathbf{Bi} = \mathbf{Bi}_{rad} \cdot \frac{\left[1 - \Phi^4\right]}{\left[1 - \Phi\right]} + \mathbf{Bi}_{conv} \tag{7}$$

where $\mathbf{Bi}$ is the total Biot number and $\mathbf{Bi}_{conv}$ and $\mathbf{Bi}_{rad}$ are the convective and radiative Biot numbers, respectively. They expresses the ratios of the heat transferred by convection to conduction, and radiation to conduction, respectively [12], and are given by

$$\mathbf{Bi}_{conv} = \frac{h_s}{\frac{\kappa}{b}} \tag{8}$$

and

$$\mathbf{Bi}_{rad} = \frac{\bar{\epsilon}_s \sigma T_s^3}{\frac{\kappa}{b}} \tag{9}$$

The Biot radiative number, $\mathbf{Bi}_{rad}$ is also called he Stark number $\mathbf{Sk}$. To obtain some idea of the expected Biot numbers for a transceiver, we assume some typical values of the parameters: $T_a = 300$ K; $T_s = 500$ K; using copper as conductive material with $\kappa = 400$ $\mathrm{Wm^{-1}K}$; and a selective coating of $\bar{\epsilon}_s = 0.06$; $h = 10$ $\mathrm{Wm^2}$, $\sigma = 5.67 \times 10^{-8}$ $\mathrm{Wm^{-2}K^{-4}}$, and $\mathbf{t} = 3 \times 10^{-3}$ m. With these values, the Biot numbers $\mathbf{Bi}_{rad} \approx 6 \times 10^{-6}$ and $\mathbf{Bi}_{conv} \approx 2.5 \times 10^{-5}$ are obtained, meaning that the conductive heat flux is by far more efficient than the radiative plus convective losses.

For systems where the Biot number is much smaller than 0.1, $\mathbf{Bi} \ll 0.1$, (as in our case), the temperatures within the body relative to the surroundings remain within 5 percent of each other. Thus, when $\mathbf{Bi} \ll 0.1$, the variation of temperature with location within the body is slight and can reasonably be approximated as being uniform, [13]. This important result will be considered in the next theoretical treatment.

From the control volume approach applied to an infinitesimal section $A_c \times dx$ in Fig. 2, where A_c is the slab cross section, which in our case is the same as the collector area $A_c = t \times l$, an energy balance on a slab element of length dx yields

$$\kappa A_c \frac{d^2T}{dx^2} dx = -P dx \left[q'' - \bar{\epsilon}_s \sigma (T^4 - T_a^4) - h_s (T - T_a)\right] \tag{10}$$

where A_c and P are the slab cross section and perimeter, respectively; $\bar{\epsilon}_s$ the average emissivity of surface s, h_s the heat transfer coefficient at the surface s, and T_a the environment temperature. Now, considering the boundary conditions:

$$T = T_o, \quad \mathbf{x} = 0 \quad ; insulated \quad wall$$

$$T = T_c, \quad \mathbf{x} = \mathbf{b} \quad ; collector \quad layer$$

Because all the heat flow is toward the collector layer located at $x = b$, (see Fig. 2), it is apparent that the maximum temperature will occur at the outer surface of the insulated wall, where $x = 0$. This leads to the adiabatic boundary condition

$$\left.\frac{dT}{dx}\right|_{x=0} = 0 \quad ; insulated \quad wall$$

Now, considering the above boundary conditions and multiplying both sides of Eq. (10) by $\left\{\frac{1}{\kappa A_c}\right\}\left\{\frac{1}{dx}\right\}\left\{\frac{dT}{dx}\right\}$, and integrating once, we obtain

$$\frac{1}{2}\left(\frac{dT}{dx}\right)^2\Big|_{x=b} = -\frac{P}{\kappa A_c}\Big\{q''(T_c-T_o) - \frac{\bar{\epsilon}_s\sigma}{5}\left[T_c^5 - T_o^5\right] + \\ +\bar{\epsilon}_s\sigma T_a^4\left[T_c - T_o\right] - \frac{h_s}{2}\left[T_c^2 - T_o^2\right] + h_s T_a\left[T_c - T_o\right]\Big\} \quad (11)$$

Taking into account our earlier discussion, where a typical transceiver is featuring very low Biot numbers, $\mathbf{Bi} \ll 0.1$, only very small thermal gradients will be present. Thus, we may make some simplifying assumptions that are valid for the transceiver. On one hand, the temperature at the collector could be expressed as a function of the maximum temperature, i.e., T_o at $x = 0$,

$$T_o = T_c + \Delta T \quad (12)$$

where ΔT is small amount, i.e., $\Delta T \to 0$. Likewise, the gradient of the temperature could be approximated by

$$\frac{dT}{dx} \approx \frac{\Delta T}{b} \quad (13)$$

where b is the length of the slab, $(T(b) = T_c)$. Then, introducing Eq. (12) into Eq. (11), and after a Taylor expansion about $\Delta T \to 0$ and neglecting the expansion terms higher than first order, we have

$$(T_c + \Delta T)^n - T_c^n \approx nT_c^{n-1}\Delta T + \cdots \quad (14)$$

and Eq. (11) becomes,

$$-\kappa\frac{dT}{dx}\Big|_{x=b} \approx \frac{P}{A_c}\Big\{q'' - \bar{\epsilon}_s\sigma(T_c^4 - T_a^4) - h_s(T_c - T_a)\Big\}\cdot b \quad (15)$$

It is interesting to see that for a transceiver featuring very low Biot numbers, the slab behaves as a system with an internal volumetric source, [14]. Then an effective volumetric source Q may be defined as

$$Q = \frac{P}{A_c}\Big\{q'' - \bar{\epsilon}_s\sigma(T_c^4 - T_a^4) - h_s(T_c - T_a)\Big\} \quad (16)$$

Although the above result was deduced mathematically, it is intuitively easy to grasp if one takes into account that the conductive heat transfer is orders of magnitude higher than radiative heat transfer. Then, all the external energy absorbed at the surface $s = P \times b$ by the slab is promptly homogeneously and volumetrically distributed inside the slab of volume $A_c \times b$.

Now, for the sake of simplicity, consider that there are no convective loses, i.e., $h_s = 0$, which implies that we are working in vacuum, i.e., the condition of solar systems pursuing high temperature receivers. In addition, if it is allowable to assume that $T_c^4 \gg T_a^4$ we have

$$Q \approx \frac{P}{A_c}\Big\{q'' - \bar{\epsilon}_s\sigma T_c^4\Big\} \quad (17)$$

and Eq. (15) yields,

$$-\kappa\frac{dT}{dx}\Big|_{x=b} = Q\cdot b \quad (18)$$

or considering the Fourier equation

$$q''_c = -\kappa\frac{dT}{dx}\Big|_{x=b} \quad (19)$$

where q''_c is the rate (per unit time) at which heat is conducted in the x-direction at a point $x = b$, i.e., at the collector. Then, Eqs. (18) and (19) result in

$$q''_c = Q\cdot b \quad (20)$$

Resolving Eq. (20), we obtain the classical distribution of temperature for a system with an internal volumetric source [14]:

$$T(\mathbf{x}) = \frac{Q}{2\kappa}(b^2 - \mathbf{x}^2) + \frac{Qb}{h_c} \quad (21)$$

where h_c is the radiative heat transfer coefficient at the collector surface, i.e., at $x = b$, which can be deduced from the following considerations. At the collector surface, the effective heat flux, q''^*_c will be equal to the heat flux leaving the collector q''^+_c, minus the heat flux coming back from the receiver, q''^-_c, or

$$q''^*_c = q''^+_c - q''^-_c \quad (22)$$

where

$$q''^+_c = \bar{\epsilon}_c\sigma T_c^4 \quad (23)$$

The fraction that strikes the receiver surface directly will be

$$q''^+_{c\to receiver} = \bar{\epsilon}_c\sigma T_c^4\cdot F_{c\to r} \quad (24)$$

where $F_{c\to r}$ is the view factor from the collector to receiver. In general, the view factor from a surface i to a surface j is denoted by $F_{i\to j}$ or just F_{ij} and is defined as *the fraction of the radiation leaving surface i that strikes surface j directly* [13]. Thus, the heat flux coming back from the receiver to the collector, q''^-_c yields,

$$q''^-_c = \bar{\epsilon}_c\sigma T_c^4\cdot F_{cr}F_{rc} \quad (25)$$

Substituting Eqs. (25) and (24) into Eq. (22), the effective heat flux at the collector yields

$$q''^*_c = \bar{\epsilon}_c\sigma T_c^4\cdot[1 - F_{cr}F_{rc}] \quad (26)$$

A radiative heat-transfer coefficient may be defined by applying the following equation

$$q''^{*}_{c} = h_c T_c \tag{27}$$

or

$$h_c = \bar{\epsilon}_c \sigma T_c^3 \cdot [1 - F_{cr} F_{rc}] \tag{28}$$

Taking into account Eqs. (17) and (28), substituting into Eq. (21) and solving for T_c yields

$$T_c = \left[\frac{q''}{[1 - F_{cr}F_{rc}]\,\bar{\epsilon}_c \frac{A_c}{Pb}\sigma + \bar{\epsilon}_s \sigma} \right]^{\frac{1}{4}} \tag{29}$$

On the other hand, the receiver temperature in the steady-state can be calculated considering the following energy balance-equation

$$A_r \bar{\epsilon}_r \sigma T_r^4 = A_c \bar{\epsilon}_c \sigma T_c^4 F_{cr} \tag{30}$$

where A_r, $\bar{\epsilon}_r$, and T_r are the area, thermal emissivity, and temperature of the receiver, respectively. Substituting Eq. (29) into Eq. (30), yields,

$$T_r = \left[\frac{q''}{[1 - F_{cr}F_{rc}]\,\bar{\epsilon}_c \frac{A_c}{Pb}\sigma + \bar{\epsilon}_s \sigma} \right]^{\frac{1}{4}} \left[\frac{A_c}{A_r} \frac{\bar{\epsilon}_c}{\bar{\epsilon}_r} F_{cr} \right]^{\frac{1}{4}} \tag{31}$$

Finally, we are primarily interested in knowing the increase of the receiver temperature using the transceiver in comparison with the classical approach. Then, a *'gain'* factor, $\mathbf{G}$, may be defined as the ratio between the receiver temperature using the transceiver, which is given by Eq. (31), and the receiver temperature without using the transceiver, called $T_{r,o}$., as

$$\mathbf{G} = \frac{T_r}{T_{r,o}} \tag{32}$$

The temperature of the receiver without using the transceiver is easily calculated as the maximum temperature attainable on the surface s, i.e.,

$$T_{r,o}^4 = \frac{q''}{\bar{\epsilon}_s \sigma} \tag{33}$$

and then, considering Eqs. (33), (32), and (31), the gain factor yields,

$$\mathbf{G} = \left[\frac{1}{[1 - F_{cr}F_{rc}]\,\frac{\bar{\epsilon}_c}{\bar{\epsilon}_s}\frac{A_c}{Pb} + 1} \right]^{\frac{1}{4}} \left[\frac{A_c}{A_r} \frac{\bar{\epsilon}_c}{\bar{\epsilon}_r} F_{cr} \right]^{\frac{1}{4}} \tag{34}$$

The above equation could be simplified considering the reciprocity rule [13] for the view factors,

$$A_i F_{ij} = A_j F_{ji} \tag{35}$$

Thus, Eq. (B5) becomes:

$$\mathbf{G} = \left[\frac{1}{\left[1 - \frac{A_r}{A_c} F_{rc}^2\right]\,\frac{\bar{\epsilon}_c}{\bar{\epsilon}_s}\frac{A_c}{Pb} + 1} \right]^{\frac{1}{4}} \left[\frac{\bar{\epsilon}_c}{\bar{\epsilon}_r} \right]^{\frac{1}{4}} [F_{rc}]^{\frac{1}{4}} \tag{36}$$

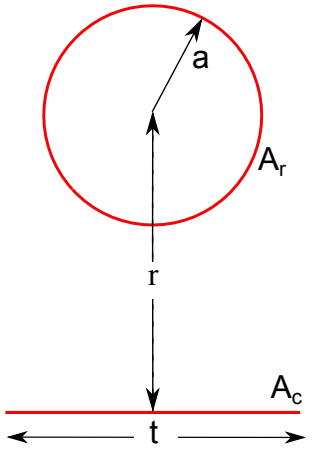

FIG. 3: Physical model for an infinitely long plane collector of finite width with a parallel infinitely long cylinder receiver

On the other hand, $\mathbf{G}$ maximises when the length of the slab increases, i.e., $b \to \infty$, yielding the following result.

$$\mathbf{G}_{max} = \left[\frac{\bar{\epsilon}_c}{\bar{\epsilon}_r} \right]^{\frac{1}{4}} [F_{rc}]^{\frac{1}{4}} \tag{37}$$

Likewise, a concentration ratio gain factor, $\mathbf{G}_c$ may be defined as (see Appendix B)

$$\mathbf{G}_c = \mathbf{G}^4 \tag{38}$$

1. *View factors*

According to Eq. (37), the enhancement in the temperature and/or concentration ratios, depends on two factors. On one hand, it depends on a material term $\left[\frac{\bar{\epsilon}_c}{\bar{\epsilon}_r}\right]$ and on the other hand, on a geometrical (or view) factor $[F_{rc}]$ between the collector and receiver.

The material term will always be the same for different designs. However, the geometrical term will depend of the specific design used.

For solar concentration technology, there are two especially important collector-receiver geometries, which should be considered, namely:

(1) A parabolic trough, which can be represented as an infinitely long plane collector of finite width with a parallel infinitely long cylinder as the receiver

and **(2)** A parabolic dish, which can be represented as an disc collector with a frontal sphere as the receiver.

For these two special important geometries, the calculated collector-receiver view factors, F_{cr}, yield the following relationships, Garg & Prakash,[3].

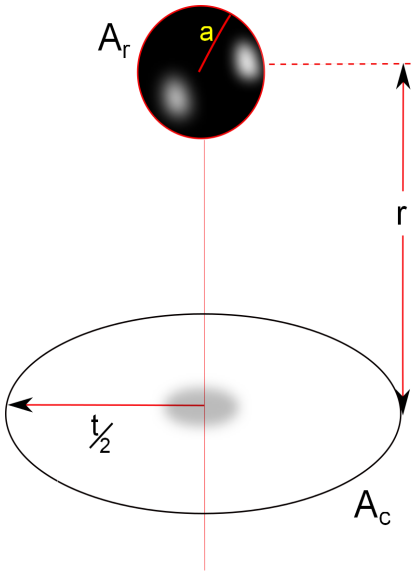

FIG. 4: Physical model for a collector disc with a frontal spherical receiver

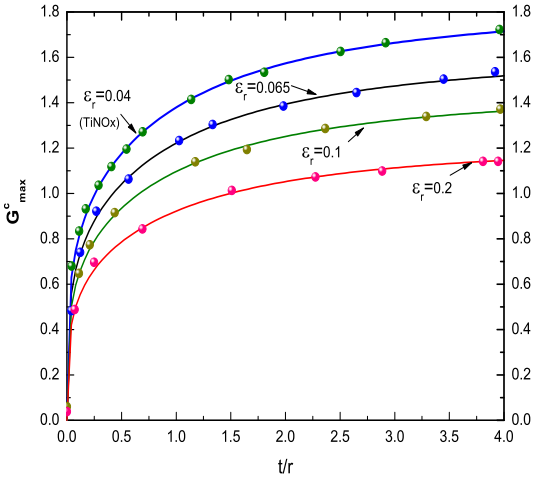

FIG. 5: Maximum gain, $\mathbf{G}^{c}_{max}$, as a function of $\frac{t}{2r}$ for a cylindrical receiver according to Eq. (37)

• **Parabolic-trough** or plane-cylinder as depicted in Fig. 3;

$$F_{cr} = \frac{2a}{t}\tan^{-1}\left(\frac{t}{2r}\right) \tag{39}$$

and

• **Parabolic dish** or disc-sphere as is depicted in Fig. 4

$$F_{cr} = \frac{8a^2}{t^2}\left[1 - \frac{1}{\sqrt{1+\left(\frac{t}{2r}\right)^2}}\right] \tag{40}$$

Inserting these view factors for cylindrical and spherical receivers in Eq. (37) we obtain the curves plotted in Figs. 5 and 6, respectively, using several emissivity values for the receiver $\bar{\epsilon}_r$ and a fixed value for the receiver $\bar{\epsilon}_c = 1$. We also assume the maximum possible receiver radius $a = r$, which represent a receiver in contact with the collector (see Figs. 3 and 4). As a matter of reference, a typical selective coating like TiNOx, used in solar technology, features an average emissivity of 0.04 at a temperature of 500°C, [15].

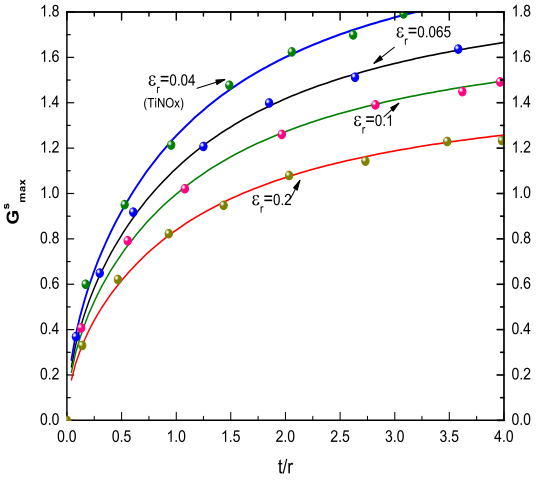

FIG. 6: Maximum gain, $\mathbf{G}^{s}_{max}$, as a function of $\frac{t}{2r}$ for a spherical receiver according to Eq. (37)

III. COMPUTER SIMULATION

A. Mathematical formulation

In this section, a simplified 2-dimensional pressure-based CFD model was developed using the commercially available CFD software Fluent. The pressure-velocity was coupled using the SIMPLEC algorithm with a first order upwind discretisation scheme for momentum and energy [16]. In order to ensure that the calculations were independent of the grid and time-step sizes, the convergence criterion was taken to be residual root-mean-square (RMS) error values of 10^{-6}. The overall imbalance in the domain was less than 1% for all variables. The convergence of the solution was checked at each time step by using the scaled residuals, defined in Fluent. The mesh resolution independence was checked by running an initial mesh and ensuring the convergence

RMS criterion of 10^{-6} and that the imbalance in the domain was less than 1%. Then, a second simulation was performed using a second mesh with finer cells throughout the domain. The simulation was run until the convergence criterion and imbalance in the domain were satisfied. The criterion for selection of the mesh was that the temperature values for two consecutive stimulations differed by less than 1%. If so, the mesh at the previous step was considered accurate enough to capture the result. Finally, the time-step independence was achieved by using time-steps of 0.5 s. A sample of the grids used in the simulations is depicted in Fig. 7.

The model consisted of a square box of width $t = 5 \times 10^{-3}$ m and length b. The length b varied between $b = 5 \times 10^{-2}$ and 1 m. The boundary conditions were calculated as follows, (see Fig. 7): the left wall was set as adiabatic, representing the insulated wall of the transceiver. The top and bottom walls were set with external emissivity coefficients equal to $\bar{\epsilon}_s = 0.04$, which is an average value for the selective coating of TiNOx [15]. The external radiation temperature (environment) was set to 300 K. The boundary condition for the right wall (collector surface) was set with an effective emissivity coefficient, $\bar{\epsilon}_{eff}$ calculated according to Eq. (26) as

$$\bar{\epsilon}_{eff} = \bar{\epsilon}_c \cdot [1 - F_{cr} F_{rc}] \tag{41}$$

The solar radiance was represented by a volumetric energy source term, S, which was included in the energy equations as

$$Q = \frac{P}{A_c} q'' \tag{42}$$

where P is the perimeter of the slab ($P = 2l + 2t$) and $A_c = t \times l$. Because $l \gg t$, the heat source was calculated as

$$Q = \frac{2}{t} q'' \tag{43}$$

For the external heat flow, q'', a generic value of $q'' = 1000$ W/m^2, simulating an average solar irradiance at the surface of Earth. The material inside the slab was copper with a thermal conductivity $\kappa = 381$ W/(mK); density, $\rho = 8978$ kg/m^3; and heat capacity, $c_p = 387.6$ J/(kgK).

The collector wall was also set with a TiNOx thermal emissivity of $\bar{\epsilon}_c = 0.04$, equal for the top and bottom surfaces.

The representative results are depicted in Figs. 8 and 9 for the heat flux at the collector and the top and bottom surfaces as a function of the length of the slab and the ratio $\frac{t}{r}$, respectively. Finally, a curve comparing the prediction given by Eq. (36) and the simulation for a slab length $b = 0.3$ m is depicted in Fig. 10. In this figure, it is easy to see that the theoretical model fits qualitatively very well with the simulations, and quantitatively with a margin of error of $\approx \pm 20\%$. The error could be associated mostly with the result of neglecting the expansion terms higher than first order in Eq. (14) or the use of a linear thermal gradient.

B. Discussion

It might be suggested that the gain obtained by using the proposed conductive focusing is because the collector is bigger than the receiver, therefore, resulting in a temperature increase. If so, there is no need to focus the heat via conduction. However, as we will see in the next important practical solar application, without the use of the proposed conductive focusing approach, the minimum size of the receiver is limited by optical physics.

IV. THE PARABOLIC SOLAR TROUGH

The most economically important solar concentrator today is the parabolic trough. A parabolic trough is a type of solar thermal collector that is straight in one dimension and curved as a parabola in the other two, lined with a polished metal mirror. The energy of sunlight that enters the mirror parallel to its plane of symmetry is focused along the focal line, where the objects to be heated are positioned. For example, food may be placed at the focal line of the trough, which causes the food to be cooked when the trough is aimed so the sun is in its plane of symmetry.

Figure 11, left-side panel, shows a classical parabolic trough system and the right-side panel shows the same system when coupled with the proposed transceiver. According to this illustrative figure, the use of the transceiver makes it possible for a smaller receiver radius to obtain higher temperatures. The reason is easy to grasp in the same figure. If the sun light is emitted directly from the collector to the receiver (as in current designs, see the left side of the figure), there is a minimum allowed radius of the receiver; if the receiver is made smaller than this radius, the solar incidence is lost. Below we will develop the mathematical treatment of the notable rays of the parabolic trough. This will allow us to provide some comparative numbers.

Figure 12 is a ray diagram of the extremal rays for the parabolic trough depicted in Fig. 11 (left-side).
According to Eq. (36), in order to know the gain in temperature $\mathbf{G}$ or in concentration ratio $\mathbf{G}_c$ we need to know the length of the transceiver b, which according to Figs. 11 and 12 correspond to the distance $\mathbf{GB}$ in these figures, i.e., $b = \mathbf{GB}$. On the other hand, the concentration ratio of the parabolic trough is easily calculated from Fig. 7, yielding:

$$C_o = \frac{\mathbf{W}}{\mathbf{CD}} = \frac{\tan(\phi + 2\theta) + \tan(\phi)}{\tan(\phi + 2\theta) - \tan(\phi)} \tag{44}$$

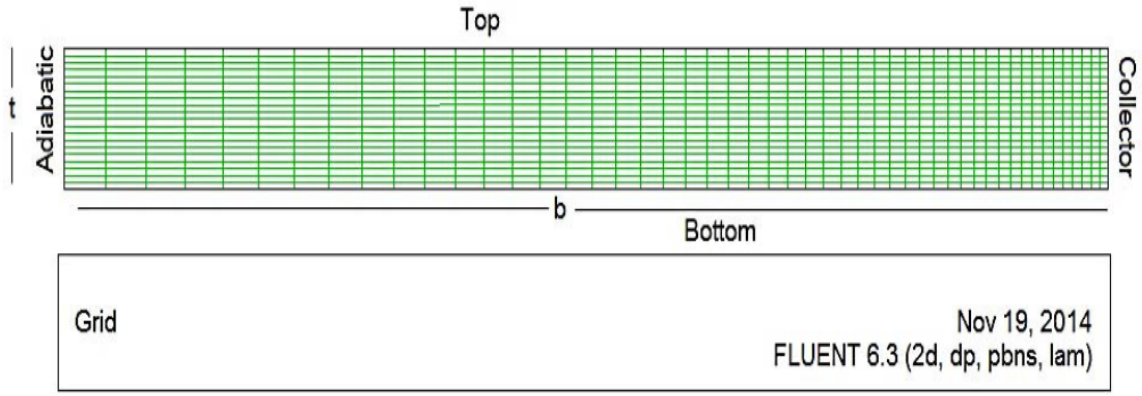

FIG. 7: A grid sample used for some computational fluid calculations

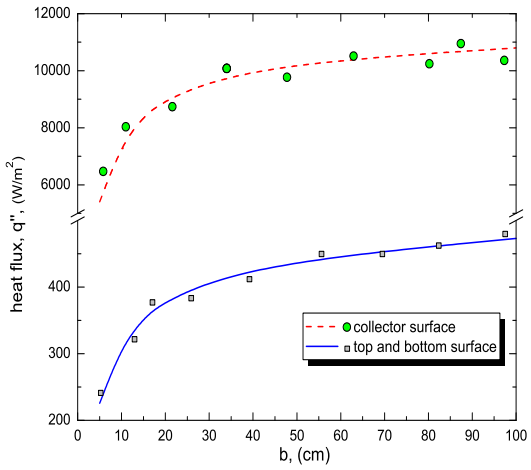

FIG. 8: The heat flux as a function of b for the top, bottom, and collector surfaces, (see Fig. 7) with $\frac{t}{r} = 1$ and $a = r$

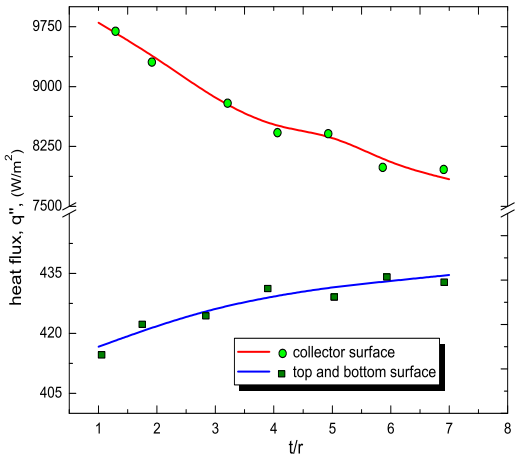

FIG. 9: The heat flux as a function of $\frac{t}{r}$ for the top, bottom, and collector surfaces, (see Fig. 7) with $b = 30$ cm and $a = r$

and the distance **GB** given by

$$\mathbf{GB} = 2\mathbf{W}\left[\frac{1}{C_o - 1}\right]\tan(\phi) \tag{45}$$

where **GB**, as previously mentioned, is the maximum length of the transceiver, b, in Eq. (36). The maximum concentration ratio C_o is obtained by differentiation of Eq. (44) and gives us $C_o = 107$ for $\phi = 45^o$. Thus, Eq. (45) becomes

$$\mathbf{GB} = b \approx \frac{\mathbf{W}}{53} \tag{46}$$

Introducing the calculated value for the length of the transceiver b, the gain **G** in Eq. (36) yields

$$\mathbf{G}_c = \left[\frac{1}{\left[1 - \frac{A_r}{A_c}F_{rc}^2\right]\frac{\bar{\epsilon}_c}{\bar{\epsilon}_s}\frac{A_c}{P}\frac{53}{\mathbf{W}} + 1}\right]\left[\frac{\bar{\epsilon}_c}{\bar{\epsilon}_r}F_{rc}\right] \tag{47}$$

A. Discussion

To obtain some idea of the shape of the curves predicted by Eq. (47), we assume some typical values of the parameters: using a selective coating for the receiver and the TiNOx surface of the transceiver, thus featuring an average emittance and absorptance of 0.04 and

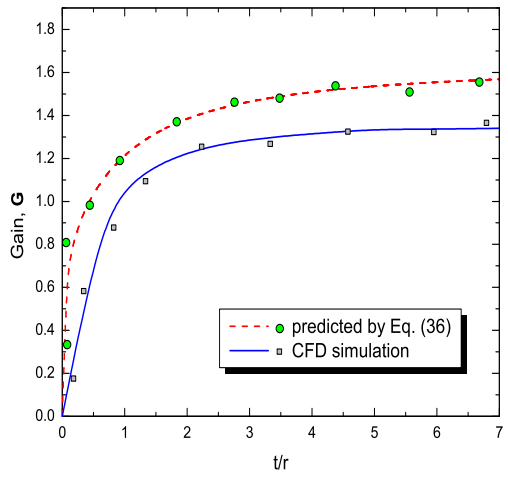

FIG. 10: The gain, **G** using $\bar{\epsilon}_r = 0.04$.

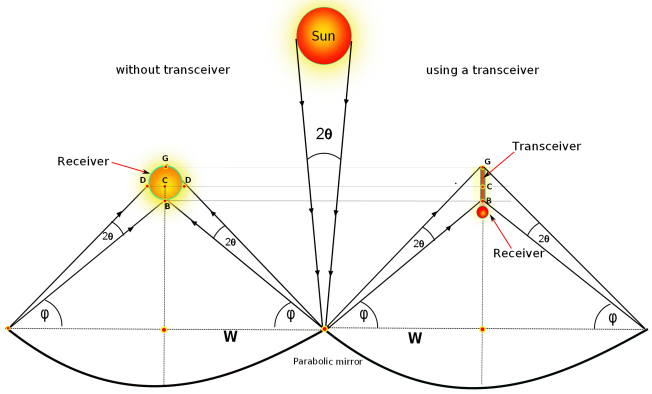

FIG. 11: The parabolic solar trough system. Left side: The classical approach. Right side: Using a transceiver.

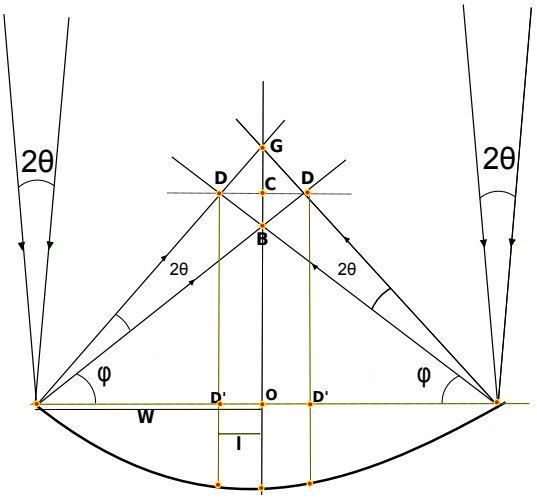

FIG. 12: Ray diagram of extremal rays from the sun incident on and reflecting of a parabolic mirror.

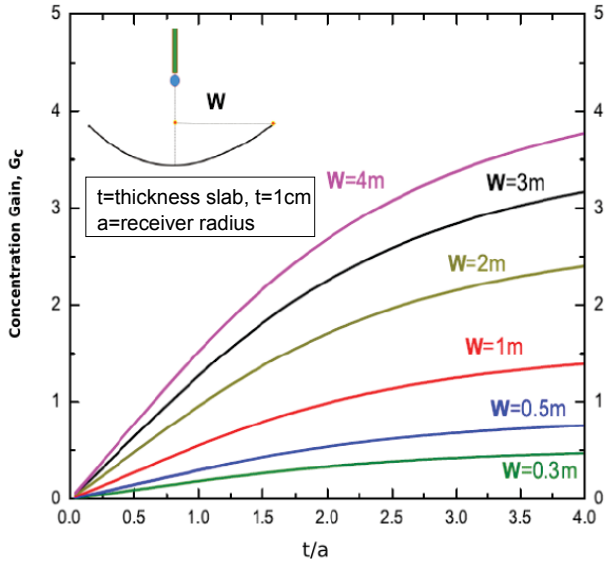

FIG. 13: The concentration gain $\mathbf{G}_c$ for a slab-thickness $t = 1$ cm as function of $\frac{t}{a}$

0.94, respectively, [15]. In addition, the maximum possible radius of the receiver was considered, i.e., $a \to r$ (see Fig. 4). The resulting curves are plotted for two different thicknesses of the slab, $t = 1$ cm (Figs. 13 and 14) and $t = 0.5$ cm (Figs. 15 and 16).

Today, typical parabolic troughs receivers have a radius $\approx 3.5cm$, i.e., **CD** = 3.5 cm (in Figs. 11 and 12). Considering the previously derived maximum concentration ratio of a parabolic trough ($C_o = 107$), Eq. (44) gives that $\mathbf{W} = \mathbf{CD} \times C_o = 374$ cm. From Figs. 14 and 16, it is seen that a concentration ratio enhancement of about 2 might be attainable for receivers with a radius close to the thickness of the transceiver.

Potential interesting applications of the proposed transceiver concept is in micro solar thermal collectors designed for example for methanol reforming for hydrogen production, [17]-[24].

V. CONCLUSIONS

In this paper, a approach for solar concentration enhancement, called thermal conductive focusing, has been proposed and discussed. We arrived at the following important conclusions:

(a) It is qualitatively reasonable to expect temperature receiver enhancements of up to 20% using conservative numbers of parameters.

(b) An analytical expression, Eq. (37), is derived that predicts the maximum attainable gain in the receiver temperature when coupling the system with a transceiver.

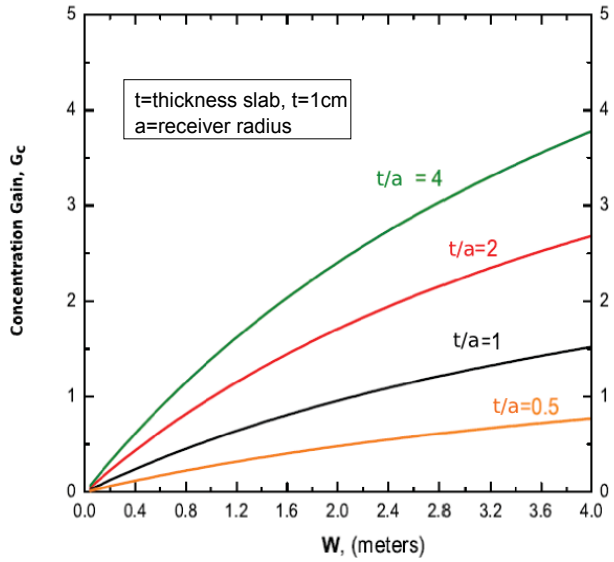

FIG. 14: The concentration gain $\mathbf{G}_c$ for a slab thickness $t = 1$ cm as function of $\mathbf{W}$

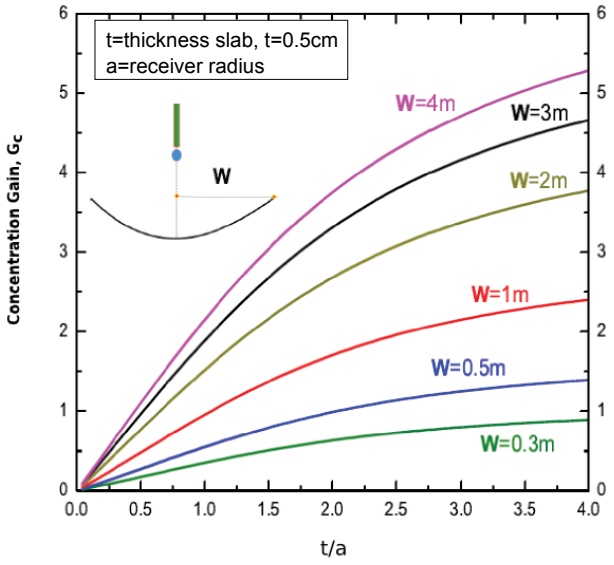

FIG. 15: The concentration gain $\mathbf{G}_c$ for a slab thickness $t = 0.5$ cm as function of $\frac{t}{a}$

(c) The derived analytical expression agrees with computational simulations within ±15%.

(d) Because conductive focusing is transporting the incident radiative flow as heat, the transceiver has the unique advantage to concentrate indistinct direct as well as diffusive radiation. This means that the approach is especially insensitive to cloudy days and also particularly attractive in applications to environments where the sun-light has a high diffusive component, for example, submarine applications or future Mars exploration missions.

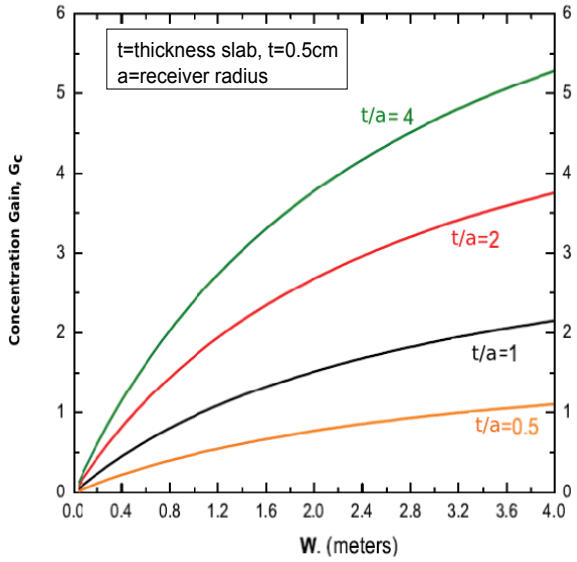

FIG. 16: The gain $\mathbf{G}$ for a slab thickness $t = 0.5$ cm as function of $\mathbf{W}$

APPENDIX A: THE EFFECT OF COLLECTOR REFLECTIVITY

For the sake of generality, assume that our collector-receiver system can be represented as two parallel layers whose facing surfaces have view factors F_{cr} and F_{rc}, respectively, and the collector layer a reflectivity ρ_c. A certain fraction of the radiation leaves the collector layer F_{cr} and enters the receiver. A fraction of this incident radiation is re-emitted to the collector. The radiation that is emitted back to the collector layer will be $F_{cr}F_{rc}$ and the radiation that is not returning to the collector will be $1 - F_{cr}F_{rc}$. Then, a fraction equal to $\rho_c F_{cr}F_{rc}$ will be reflected back to the receiver again. Due to this process of back and forth reflection, a steady state results giving that the total proportion of radiation entering the receiver (from the collector) is:

$$(1 - F_{cr}F_{rc}) \sum_{n=0}^{\infty} F_{cr}^n F_{rc}^n \rho_c^n \tag{A1}$$

Considering that F_{cr}, F_{rc}, and ρ_c are < 1, the series converges as

$$\frac{1 - F_{cr}F_{rc}}{1 - F_{cr}F_{rc}\rho_c} \tag{A2}$$

Thus, the correction factor in the effective heat flux leaving the collector can be introduce in Eq. (26) yielding,

$$q''^*_c = \bar{\epsilon}_c \sigma T_c^4 \cdot \frac{1 - F_{cr}F_{rc}}{1 - F_{cr}F_{rc}\rho_c} \tag{A3}$$

and the radiative heat-transfer coefficient c corrections given by

$$h_c = \bar{\epsilon}_c \sigma T_c^3 \cdot \frac{1 - F_{cr}F_{rc}}{1 - F_{cr}F_{rc}\rho_c} \tag{A4}$$

where, of course in the limit $\rho_c \to 0$, we recover the previous expression, Eq. (28). Proceeding in the same way as in the previous section, it is easy to demonstrate that the new gain, $\mathbf{G}$ corrected by the collector reflectivity, yields

$$\mathbf{G} = \left[\frac{1}{\left[\frac{1-\frac{A_r}{A_c} F_{rc}^2}{1-\frac{A_r}{A_c} F_{rc}^2 \rho_c} \right] \frac{\bar{\epsilon}_c}{\bar{\epsilon}_s} \frac{A_c}{Pb} + 1} \right]^{\frac{1}{4}} \left[\frac{\bar{\epsilon}_c}{\bar{\epsilon}_r} F_{rc} \right]^{\frac{1}{4}} \tag{A5}$$

and the maximum gain, i.e., when $b \to \infty$, by the same Eq. (37)

$$\mathbf{G}_{max} = \left[\frac{\bar{\epsilon}_c}{\bar{\epsilon}_r} F_{rc} \right]^{\frac{1}{4}} \tag{A6}$$

APPENDIX B: CONCENTRATION GAIN $\mathbf{G}_c$

Similar to the previous sections, a gain concentration ratio may be defined as follows. If we define the total concentration ratio C (using the transceiver) as the product of the concentration ratio without using the proposed transceiver, C_o, and a gain factor $\mathbf{G}_c$ we have

$$C = C_o \cdot \mathbf{G}_c \tag{B1}$$

where $\mathbf{G}_c$ is the concentration ratio gain factor, defined as

$$\mathbf{G}_c = \frac{C}{C_o} \tag{B2}$$

On the other hand, the external solar heat flux on the transceiver q'' is the product of the solar flux q''_o multiplied by the concentration ratio C_o. Thus, q'' can be written as

$$q'' = q''_o C_o \tag{B3}$$

and the following relationship is valid

$$\bar{\epsilon}_r \sigma T_r^4 = q''_o C_o \cdot \mathbf{G}_c \tag{B4}$$

which, considering Eqs. (31) and (B3) gives

$$\mathbf{G}_c = \mathbf{G}^4 \tag{B5}$$

and

$$\mathbf{G}_{max,c} = \mathbf{G}_{max}^4 \tag{B6}$$

NOMENCLATURE

a = radius of receiver, (m)
A = area, (m^2)
b = slab length, (m)
Bi = Biot number
F = view factor
$\mathbf{G}$ gain factor
h = convective heat transfer coefficient, (W/m^2K)
l = slab width, (m)
P = slab perimeter, (m)
q'' = heat flux, (W/m^2)
Q = volumetric energy source, (W/m^3)
r = distance from the surface of the collector to the centre of the receiver, (m)
S = energy source, W/m^3
t = slab thickness, (m)
T = temperature, (K)
V = volume (m^3)
x = longitudinal coordinate (m)
z = transversal coordinate (m)

Greek symbols

σ = Stefan-Boltzmann constant
ρ = reflectivity
κ = thermal conductivity
Φ = non dimensional number defined by Eq. (6)

Subscripts, Superscripts

a = environment
c = collector
$conv$ = convection
cr = collector $\to$ receiver
rad = radiative
rc = receive r$\to$ collector
$effec$ = effective value
s = slab or incident surface
max = maximum
r = receiver
ν = frequency (s^{-1})
o = at the adiabatic wall, or initial value
$+$ = radiation leaving surface of collector
$-$ = radiation coming back from the receiver to the collector

ACKNOWLEDGEMENTS

This work was developed during a postdoctoral scholar visit at the Royal Melbourne Institute of Technology and National University of Australia at Canberra in Australia. The author is indebted to Prof. Gary Rosengarten and Prof. John Pye at the Royal Melbourne Institute of Technology and National University of Australia at Canberra, respectively, for their support as well for many helpful, encouraging, and stimulating discussions that led to an understanding of the present problem and the state-of-the-art in solar concentrators. This work was performed under a Grant Ramon y Cajal of the Ministerio de Economia y Competitividad of the Spain Government RYC-2013-13459.

REFERENCES

[1] Lovegrove, K, Stein, W. Concentrating solar power technology. Principles, developments and applications. Woodhead Publishing in Energy.

[2] Francis De Winter. Solar Collectors, Energy Storage, and Materials. The MIT Press. June 21, 1991.

[3] Garg H.P., Prakash, J. Solar Energy: Fundamentals and Applications. tata McGraw-Hill Publishing Company Limited. 1997

[4] Max Planck. A survey of Physical Theory. Dover Publications. Inc, New York. 1960. Chapter, The unit of the Physical Universe, p.p. 19.

[5] Wang Fuqiang., Tan Jianyu., Yong Shuai, Tan Heping., Chu Shuangxia. 2014. Thermal performance analysis of porous media solar receiver with different irradiative transfer models. International Journal of Heat and Mass Transfer, Volume 78, 7-16

[6] Chih-Cheng Chen, Po-Chuan Huang Numerical study of heat transfer enhancement for a novel flat-plate solar water collector using metal-foam blocks. International Journal of Heat and Mass Transfer, Volume 55, 23-24, (2012), 6734-6756

[7] Po-Chuan Huang, Chih-Cheng Chen, Hsiu-Ying Hwang. Thermal enhancement in a flat-plate solar water collector by flow pulsation and metal-foam blocks. International Journal of Heat and Mass Transfer, Volume 61, (2013), 696-720

[8] Wang Fuqiang., Yong Shuai., Tan Heping , Yu Chunliang. 2013. Thermal performance analysis of porous media receiver with concentrated solar irradiation. International Journal of Heat and Mass Transfer, Volume 62, 247-254

[9] O. Garcia-Valladares, N. Velazquez Numerical simulation of parabolic trough solar collector: Improvement using counter flow concentric circular heat exchangers. International Journal of Heat and Mass Transfer, Volume 52, 3-4, 31, (2009), 597-609

[10] Chih-Cheng Chen, Po-Chuan Huang. Numerical study of heat transfer enhancement for a novel flat-plate solar water collector using metal-foam blocks.*International Journal of Heat and Mass Transfer*, Volume 55, 23-24, (2012), 6734-6756

[11] Po-Chuan Huang, Chih-Cheng Chen, Hsiu-Ying Hwang. Thermal enhancement in a flat-plate solar water collector by flow pulsation and metal-foam blocks. *International Journal of Heat and Mass Transfer*, 61, (2013), 696-720

[12] J. Kunes. Dimensionless Physical Quantities in Science and Engineering. Elsevier (2012).

[13] Y.A. Çengel, A.J. Ghajar. Heat and Mass Transfer, Fundamentals & Applications. Fourth Edition. McGraw Hill (2007)

[14] S. Glasstone. Principles of Nuclear Reactor Engineering. D. Van Nostrand Company, Inc.; 1st edition (1955)

[15] C.E. Kennedy. Review of Mid-to-High Temperature Solar Selective Absorber Materials. National Renewable Energy laboratory.NREL. NREL/TP-520-31267. 2002

[16] Ansys Fluent. 6.3. Theoretical guide.Solidification and melting. 2009

[17] X. Gua., R.A. Taylor., Q. Lia., J.A. Scott., G. Rosengarten. 2015. Thermal analysis of a micro solar thermal collector designed for methanol reforming. Solar Energy. 113, 189-198

[18] C. Stanley., A. Mojiri,, M. Rahat., A. Blakers., G. Rosengarten. 2016. Performance testing of a spectral beam splitting hybrid PVT solar receiver for linear concentrators. Applied Energy, 168, 303-313

[19] M. Rahou, A. Mojiri, G. Rosengarten., J. Andrews. Optical design of a Fresnel concentrating solar system for direct transmission of radiation through an optical fibre bundle. Solar Energy, 124. 15-25

[20] A. Mojiri, C. Stanley, D. Rodriguez-Sanchez, V. Everett, A. Blakers, G. Rosengarten. 2016. A spectral-splitting PV-thermal volumetric solar receiver. Applied Energy, 169. 63-71

[21] Q. Li., A. Shirazi., C. Zheng., G. Rosengarten., J.A. Scott., R.A. Taylor. 2016. Energy concentration limits in solar thermal heating applications. Energy, 96, 253-267

[22] N. Karwa, L. Jiang., R. Winston., G. Rosengarten. 2015. Receiver shape optimization for maximizing medium temperature CPC collector efficiency. Solar Energy, 122, 529-546.

[23] D. Rodriguez-Sanchez, G. Rosengarten. 2015. Improving the concentration ratio of parabolic troughs using a second-stage flat mirror. Applied Energy. 159, 620-632

[24] H. Wang., V.P. Sivan., A. Mitchell., G. Rosengarten., P. Phelan., L. Wang. 2015. Highly efficient selective metamaterial absorber for high-temperature solar thermal energy harvesting. Solar Energy Materials and Solar Cells. 137, 235-242